



Monitoring of HR and BP using DFT and Pan-Tompkins Algorithm

Muhammed Siyad S, Thasni N, Rajeswary M

Department of Electronics and Communication Engineering, Musaliar college of Engineering Chirayinkeezhu ,
Trivandrum, Kerala, India

ABSTRACT

In this paper we propose monitoring of blood pressure and heart rate using Discrete Fourier Transform and Pan-Tompkins algorithm to achieve higher wear ability and high accuracy. Motion artifacts induced by the head movements are dealt with machine learning framework to enable practical application scenarios. Here we suggest to place all the electrocardiogram (ECG) and photoplethysmography (PPG) sensors behind two ears to successfully acquire weak ear -ECG/PPG signals using a semi customized platform. After introducing head motions towards, we apply an unsupervised learning algorithm, Pan Tompkins to learn and identify raw heartbeats from motion artifacts compacted signals. Furthermore, we propose another unsupervised learning algorithm to filter out distorted/faking heartbeats, for the estimation of ECG to PPG pulse transit time (PTT) and HR. Specifically, we introduce a Discrete Fourier Transform (DFT) to quantify distortion conditions of raw heartbeats referring to a high-quality heartbeat pattern, which are then compared with a threshold to perform purification. The heartbeat pattern and the distortion threshold are learned by a K-medoids clustering approach and a histogram triangle method, respectively. Afterwards, we perform a comparative analysis on ten PTT or PTT&HR-based BP learning models.

Keywords: Electrocardiogram (ECG), Photoplethysmography (PPG), Pulse Transition Time (PTT), Machine Learning, Signal Processing, Pan Tompkins algorithm, Discrete Fourier Transform.

I. INTRODUCTION

High blood pressure increases the risk of disease and death in the population. As a clinical risk factor it is of major public health importance and compared to other leading risk factors accounts for the third largest proportion of disability adjusted life years lost globally after dietary factors and cigarette smoking. Blood is circulated through the body by the heart, and the beating of the heart leads to peaks and troughs in blood pressure. The peaks are called systolic and the troughs diastolic. Blood pressure is measured as systolic/diastolic, e.g. 140/90 mmHg (pressure equivalent of millimeters of mercury). Blood pressure varies normally from minute to minute, and over days and weeks, but a consistently raised blood pressure increases the risk of certain

diseases. Cardiovascular risk increases above values of 115/70, but blood pressure persistently above 140/90 mmHg is accepted as an appropriate reason to consider treatment. The measurement of blood pressure is an important consideration because it requires a certain level of skill, an appropriate setting and well maintained and calibrated equipment. A measurement should be based on at least two reading.

High blood pressure increases the risk of a range of diseases: coronary heart disease (angina, heart attack), stroke (both that due to a blood clot and that due to bleeding), heart failure (heart strain - especially left ventricular), aortic aneurysm (dilated aorta with risk of rupture and massive internal haemorrhage), peripheral vascular disease (reduced blood supply to

the limbs), chronic kidney disease (including renal failure), retinal disease (visual impairment).

Typical values for a resting healthy adult human are approximately 120 mmHg (16 kPa) systolic and 80 mmHg (11 kPa) diastolic written as, 120/80 mmHg. These measures of arterial pressure are not static, but undergo natural variations from one heartbeat to another and throughout the day, they also change in response to stress, nutritional factors, drugs, or disease. The Table 1 shows the normal healthy Blood Pressure ranges for adults aged 18 and older.

The values of Blood Pressure vary significantly during the course of 24 hours according to an individual's activity. Basically, three factors namely, the diameter of the arteries, the cardiac output and the state or quantity of blood are mainly responsible for the Blood Pressure level. Table 1. Age related Blood Pressure range

Table 1. Age Related Blood Pressure Range

Age related normal healthy blood pressure range						
Age	Systolic BP (mmHg)			Diastolic BP (mmHg)		
	Mini	Average	Maxi	Mini	Average	Maxi
15 to 19	105	117	120	73	77	81
20 to 24	108	120	132	75	79	83
25 to 29	109	121	133	76	80	84
30 to 34	110	122	134	77	81	85
35 to 39	111	123	135	78	83	86
40 to 44	112	125	137	79	83	87
45 to 49	115	127	139	80	84	88
50 to 54	116	129	142	81	85	89
55 to 59	118	131	144	82	86	90
60 to 64	121	134	147	83	87	91

Wearable computers are paving a promising way for pervasive smart health wearables for people around the world, especially for developing worlds where major problems include lack of health infrastructure and limited health coverage. They can provide health management in a more affordable manner than traditional health services, especially when long-term continuous health data collection is needed for effective diagnosis/treatment of chronic diseases like hypertension. Many investigations in wearable BP monitoring have been reported and summarized in several recently published surveys.

The most popular BP estimation theories are based on the fact that BP is often reversely correlated with the pulse transit time (PTT), i.e., the blood wave propagation time between two arterial sites. In the arterial vessel, a higher BP usually generates a higher velocity of propagation, which results in a smaller time (i.e. PTT) for the wave to travel along the vessel, and vice versa. To measure the PTT start and end time, the electrocardiography (ECG) and photoplethysmography (PPG) signals are the most widely used ones. The ECG heartbeat peak corresponds to the pressure wave occurrence time on the proximal site, i.e., the thoracic aorta, and thus can represent the PTT start time. The PPG heartbeat foot corresponds to when the pulse arrives the distal site, i.e., the location where the PPG sensor is placed, and thus can reflect the PTT end time. In these works, the most frequently applied ECG/PPG sensors placement methods are two-wrists/finger, chest/finger, and chest/chest.

However, these placement approaches may impact the wearability and comfortableness, considering the former two require extra connection overhead or wearing more than one device, and the last one may need a chest strap to fix the sensors and suffer from sweating. Some works proposed an in-ear PPG signal monitor to measure HR and other information, but they did not acquire ECG signal and measure BP. Another work proposed placing the PPG sensor behind the left ear and placing two ECG electrodes behind the left ear and neck, respectively. However, the signal quality may be impacted if the collar coat touches the electrode on the neck in long-term daily applications. Moreover, this work did not evaluate the BP estimation performance after obtaining the PTT measurements, and did not consider daily movements-induced motion artifacts.

Another significant concern lacking of enough attention and study is whether BP estimation systems can tolerate to large amounts of motion artifacts, since the body movements in long-term daily

applications inevitably induce time varying skin-sensor contact variations which usually impact or even corrupt the ECG and PPG signals acquired. The accelerometers can be applied to track the motion information, which can be used as a reference for motion artifacts removal, such as discarding signal periods or adaptive filter-based motion artifact cancellation.

Moreover, there are diverse BP modeling theories and strategies being studied, to deal with the underlying complicated blood pressure wave generation and propagation mechanisms, nevertheless, the comparative analysis of major BP models is rather limited. One thing worth noting is that, we have previously reported a single-arm-worn ECG&PPG-based blood pressure monitors which can provide a super wearability, but in this study we focus on another novel easy-wearing blood pressure

monitor with novel sensor placement methods. Besides, body movements during blood pressure estimation were not considered in our previous work, however, in this study, we have made lots of efforts to deal with motion artifacts towards all-day application scenarios. One new effective method is need for solving these problems.

II. METHODS AND MATERIAL

A. System Overview

The proposed machine learning-enabled system is illustrated in Figure 1. The top part (Figure 1a) gives the customized hardware prototype and the sensors placement method for ear-ECG and PPG signals acquisition. The bottom part (Figure 1b)

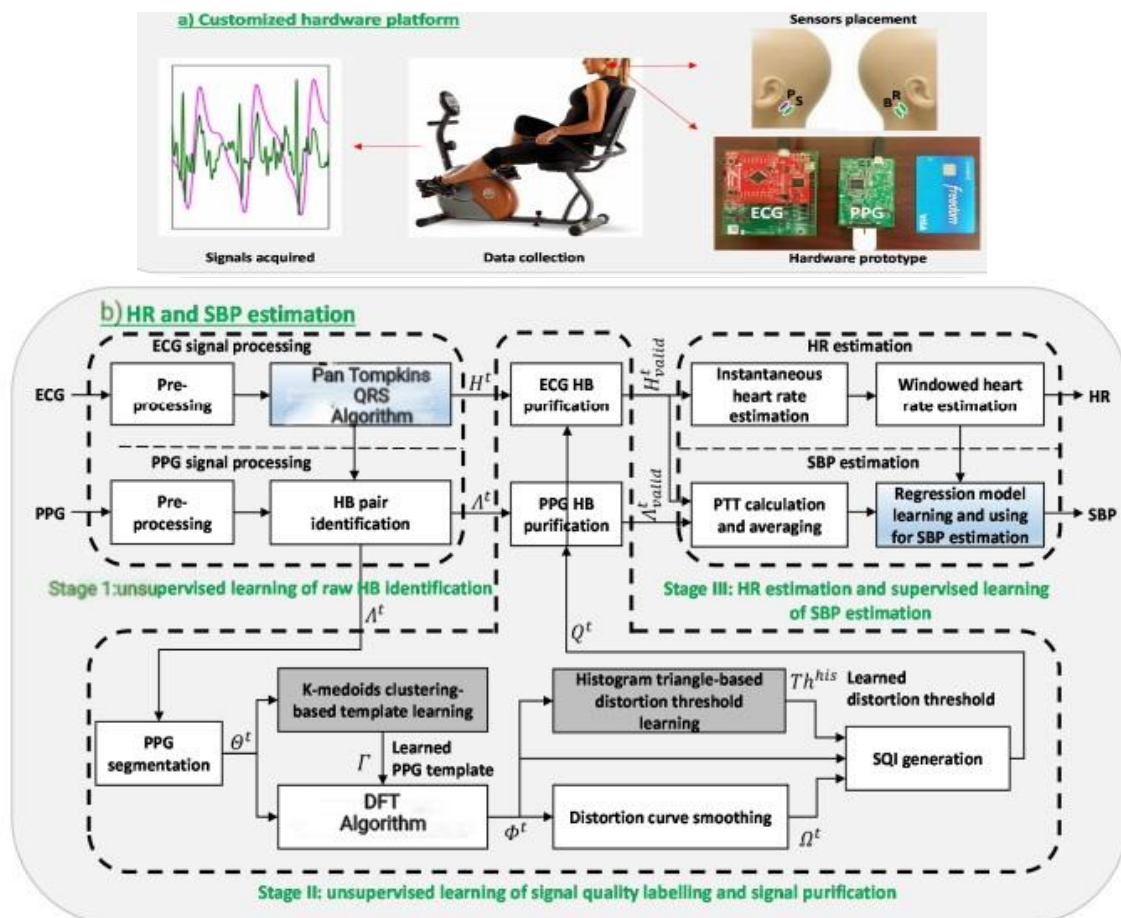


Figure 1. The proposed wearable cuff-less SBP and HR monitoring from motion artifacts-sensitive ear-ECG/PPG signals.

shows the flow of the signal processing and HB/SBP estimation algorithm including three stages, i.e., stage I – supervised learning of heartbeat (HB) identification, stage II – unsupervised learning of signal quality labelling and signal purification, and stage III – HR estimation and supervised learning of SBP estimation. The proposed algorithms can be run on the mobile devices such as cellphones. Therefore, no computation resources will be introduced to the wearables and the form factor will not be increased. One thing worth noting is that the ML-based algorithms are expected to deal with large amounts of motions artifacts in daily applications, which is very challenging but necessary to enable 24-hour continuous blood pressure/heart rate tracking.

B. Customized Hardware Platform and Sensors Placement.

The customized hardware platform shown in Figure 1a includes two parts, i.e., the ECG and PPG subsystems. In the former one, the ECG signal is acquired by an ADS1299 24-bit analog-to-digital (ADC) with a sampling rate of 500 Hz on a TI ADS1299EEG-FE evaluation board (green one) and is then sent through the SPI port to a TI Tiva™ C series LaunchPad (red one), which is equipped with an ARM Cortex M4 microcontroller to configure the ADC and relay the signal to a PC via the USB port. In the latter one, the PPG signal is acquired by a 22-bit ADC with a sampling rate of 128 Hz on a TI AFE4490SPO2 evaluation board, which also owns an MSP430F5529IPN microcontroller to configure the ADC and relay the data to the PC. A higher sampling rate for ECG is based on the consideration that it is used for both HR and PTT estimation. This prototype can be conveniently used in long-term applications after removing evaluation-specific components and adding a wireless module.

The sensors placement method proposed is illustrated in the top right part of Figure 1a, where the R/B/S

correspond to the reference/bias/signal electrodes for single-lead ECG acquisition, and P represents the sensor for PPG measurement. All the sensors can be integrated into glasses or ear headsets to achieve a much higher wearability and comfortableness, compared with the chest or wrists placement.

C. Dataset Recording

The customized platform was applied to acquire an ear ECG/PPG dataset from fourteen subjects, to evaluate the effectiveness of the proposed proof-of-concept system. The data collection was approved by the university IRB office and the informed consent was obtained from all participants. The data collection comprises a thirty-minute training session and a thirty-minute testing session for each subject. Each session can be further split to fifteen two-minute trials. During the first seven trials, the subject stayed still to get low SBP conditions, and during each of the other eight trials, the subject rode a recumbent exercise bike in the first minute and stayed still in the second minute, to perturb the SBP to a larger range similar to the methods used in many studies.. The reference SBP, denoted as SBP_{cuff}, was measured on the left arm in the second minute of each trial, using an ambulatory BP monitor CONTEC ABPM5. Correspondingly, the ear signals in the second minute of each trial are used for HR and SBP estimation. The chest-ECG signal was also collected to obtain the ground truth of heartbeat occurrence time.

One thing worth noting is that deleting time periods with distortions may over-discard signal periods which are still of an acceptable signal quality. It means that there may still be a portion of good heartbeats during a signal period with distortions. So, it may be helpful to provide a high temporal resolution of BP estimates (we aim to report minute-level BP), if the good heartbeats can be extracted from all signal periods based on beat-specific quantitative distortion values. We notice that the ear signals are frequently impacted by

motion artifacts, even the users take a sitting or standing position, there are still lots of motion artifacts, such as continuous background motion artifacts due to uncontrolled neck muscle and blood vessels movements, and motion artifacts induced by little head movements such as slightly looking around or up and down. Taking practical scenarios into account, we further introduced much severer motion artifacts by performing head movements including shaking the head and nodding for one third of each signal period. Specifically, in the second minute of each trial, the subject was asked to shake the head during the first ten seconds and nod during the fourth ten seconds. These head movements corrupt a large portion of signals and make heartbeat identification much more challenging. Therefore, it is necessary to utilize lots of signal periods even distorted by motion artifacts to guarantee the high-resolution BP tracking.

D. Unsupervised Learning of HB Identification

The stage I of the proposed algorithm in Figure 1b performs raw heartbeat identification from both pre-processed ear-ECG and PPG signals. Considering the ECG signal is of relatively richer signal characteristics (especially the QRS complex) than the PPG signal we firstly introduce an advanced unsupervised machine learning approach for raw ECG heartbeats identification, based on which the raw PPG heartbeat pairs are then determined by a minima searching method.

1) Signal Pre-processing

The raw ear-ECG and PPG signals are both processed by a six-order Butterworth bandpass filter (2-30 Hz and 0.5-8 Hz, respectively). Then PPG is resampled to 500 Hz to obtain a same time resolution as ECG. More analysis about the signal quality with deliberately introduced severe motion artifacts will be given later.

2) ECG-based and PPG-based Heartbeat Identification

To identify raw heartbeats from weak ear-ECG signal impacted or corrupted by large amounts of

background and deliberately introduced motion artifacts, our previously reported Pan Tompkins algorithm is applied. An analog filter bandlimits the ECG signal at 50 Hz. An analog-to-digital converter (ADC) samples the ECG at a rate of 200 samples/s. The resulting digital signal passes successively through a sequence of processing steps that includes three linear digital filters implemented in software. First is an integer coefficient bandpass filter composed of cascaded low-pass and high-pass filters. Its function is noise rejection. Next is a filter that approximates a derivative. After an amplitude squaring process, the signal passes through a moving-window integrator. Adaptive thresholds then discriminate the locations of the QRS complexes.

E. Unsupervised Learning of Signal Quality Labelling and Signal Purification (SQLSP)

Considering that large amounts of back ground and head movements-induced motion artifacts usually severely corrupt a large portion of weak ear signals, many highly distorted or faking heartbeats in some signal segments need to be suppressed. Therefore, an unsupervised learning approach is proposed to automatically purify the raw heartbeats, as shown in stage II of the proposed algorithm in Figure 1b. Two major considerations made here include: 1) choosing an unsupervised learning strategy not a supervised one, and 2) further learning motion artifacts-sensitive behaviors of raw PPG heartbeats not ECG heartbeats. The former one is based on the finding that it is hard to generate ground truth signal quality labels for raw heartbeats (e.g., labelled as a good or poor quality level when using a binary labelling method) which are necessary for supervised signal quality learning. Firstly, the background motion artifacts induced by uncontrolled neck muscle and blood vessels movements, especially with exercise stress, usually occur randomly making it difficult to manually label the signal quality for raw heartbeats.

Moreover, the head movements deliberately introduced (shaking and nodding) to generate more critical motion artifacts cannot be strictly control. Therefore, we propose an unsupervised learning approach to automatically label the signal quality after self-learning the diverse behaviors of raw heartbeats corrupted by motion artifacts. Further learning motion artifacts-impacted behaviors of raw PPG heartbeats is based on the observation that the PPG signal is of less signal characteristics and thus more sensitive to motion artifacts than the ECG signal. Therefore, the difference between high quality and low quality raw PPG heartbeats is more learnable for an unsupervised learner. Firstly, the PPG stream is split to raw PPG heartbeat segments (s1-segmentation), which are then fed to a K-medoids clustering-based learner to determine a high quality heartbeat template (s2-template learning). Afterwards, the learned template is used to screen the raw PPG heartbeats to quantify the degree of distortion based on the DTW approach (s3-HB distortion), which can effectively measure the dissimilarity between raw heartbeats owning time varying length/morphology and the learned template using a dynamic programming strategy. The distortion values measured are used to learn by a histogram triangle-based method a distortion threshold (s4-threshold learning), which can be applied to generate binary heartbeat-specific signal quality indices for heartbeat purification purpose (s5-s8).

1) PPG Segmentation

The PPG stream is segmented based on the raw PPG heartbeat locations identified.

2) K-medoids Clustering-based Template Learning

A PPG heartbeat template with a good morphology is needed by the DFT algorithm, to screen the raw PPG heartbeats to calculate their distortion values used in signal quality labelling. However, there is no pre-labeled signal quality information to directly perform PPG template

selection, otherwise, it is unnecessary to perform the unsupervised learning of signal labelling in the proposed system. It is known that when there are more motion artifacts, there is also more morphological randomness in the raw heartbeats, which results in a decreasing consistency among them. If we partition the raw heartbeats into different groups according to beat-to-beat consistency, the high quality heartbeats are more likely to be clustered together benefitting a better inter-beat consistency, and the low quality heartbeats tend to be partitioned into multiple clusters due to much more diverse motion artifacts-induced morphologies. Based on this consideration, a K-medoids clustering approach is introduced to learn a good PPG template from the raw heartbeats. K-medoids clustering is a classical unsupervised machine learning algorithm which breaks the objects (raw heartbeats) up into clusters and attempt to minimize the distance (consistency) between objects belonging to a cluster and the representative object designated as the center (medoid) of that cluster. Therefore, the medoid that represents a highest number of objects is selected as the high quality PPG heartbeat template. Moreover, also to lower the computation load, the Euclidean distance is chosen to measure inter-object distance. Since the time-varying raw heartbeats are usually of different lengths, they are all resampled to own a length of 9, which is the averaged length of all raw heartbeats in, to enable the Euclidean distance calculation.

3) Histogram Triangle-based Distortion Threshold Learning

Based on quantified distortion evaluation of the raw PPG heartbeats, the next is to learn an appropriate distortion threshold to differentiate heartbeats with a good or a poor quality. The same consideration used in K-medoids clustering-based template learning is applied here, i.e., low quality raw heartbeats owning much more diverse distorted morphologies due to random motion artifacts. Therefore, statistically, in a distortion histogram,

the raw heartbeats with a relatively good quality should concentrate in the low distortion area (the left side of the x-axis), while the ones with gradually worse signal quality conditions usually spread over the higher distortion area (the middle and right side of the x-axis), due to poor consistency induced by random motion artifacts. Leveraging this interesting left-skewed histogram, we use an unsupervised learning approach called histogram triangle method to learn the distortion threshold

4) Distortion Curve Smoothing

To further enhance the robustness before separating the raw PPG heartbeats to binary groups with a good or poor signal quality levels, the raw PPG heartbeats distortion values are smoothed by a 10th order moving average method. This is based on the consideration that when some raw PPG heartbeats own high distortion values, they are either real heartbeats highly corrupted by severe motion artifacts, or motion artifacts-induced interferential spikes. Therefore, their neighboring raw PPG heartbeats with lower distortion values may also have a high possibility to be impacted by motion artifacts. The smoothing operation can elevate the low distortion values for these neighboring heartbeats, and help cluster raw heartbeats in suspicious time periods to the low signal quality group more strictly.

5) SQI Generation

Based on the learned distortion threshold and the smoothed distortion curve, the raw PPG heartbeats can now be clustered to binary groups with a good or poor quality level. Firstly, although the smoothed distortion curve V in the trial can help elevate low distortion values when they are close to high distortion values (i.e., suspicious time periods), the smoothing operation usually lowers the high distortion values at the same time. It means that the unsmoothed distortion curve C can still contribute to highlight the heartbeats with high distortion values. Therefore, we compare not only the

smoothed distortion curve but also the unsmoothed one to the learned distortion threshold ST for the SQI set generation. Secondly, the motion artifacts due to time-varying electrode-skin contact variations are so random that it is impractical to cover all motion artifacts scenarios in the training session. If there happen to be some severe motion artifacts resulting in very high distortion values in the testing session, they may over-elevate many low distortion values in the corresponding suspicious time periods. Consequently, this strict SQI generation procedure may filter out too many raw heartbeats in some trials. However, based on our observation, even after aggressively introducing twenty-second head movements-induced motion artifacts in each trial (the subjects are usually asked to stay during estimation, but we aggressively asked them to perform movements for one third of each trail time), the heartbeats corrupted are still lower than fifty percent. Leveraging this observation, we introduce a heartbeats protection strategy to protect the best heartbeats in each trail, by adaptively increasing the learned threshold ST with a step size of \ast (1%) until at least heartbeats are labeled with a good quality level. To guarantee the consistency of the proposed SQI generation algorithm, this protection operation is also applied to the training session. The BP estimate quality indicator is also reported to reflect the percentage of raw heartbeats left after step 2 but before heartbeat protection. The indicator can be used to select out high confident BP estimates according to specific application requirements, After strictly labelling low quality raw PPG heartbeats and performing necessary heartbeats protection operations, the generated SQI set based on raw PPG heartbeats can now be used for heartbeats purification.

6) PPG and ECG Heartbeats Purification.

Considering there are still many residual highly corrupted and faking heartbeats, both raw ECG and PPG heartbeats are purified according to the SQI information, i.e., filtering raw heartbeats with an SQI

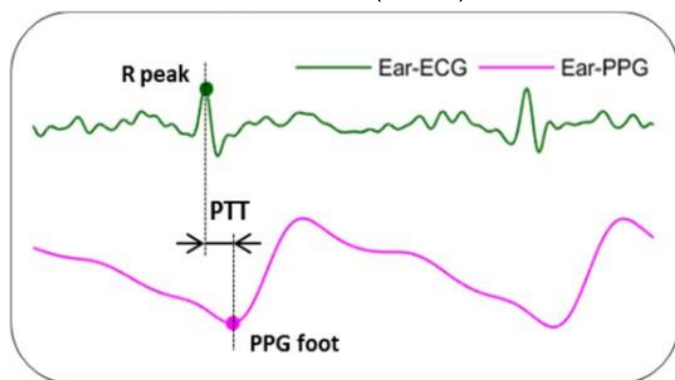
of 0 and keeping those with an SQI of 1. The purified heartbeats are then sent to the stage III of the proposed HR and SBP estimation algorithm.

F. HR Estimation and Supervised Learning of SBP

Estimation Based on the purified ECG heartbeats, the HR estimates can now be achieved, and together with purified PPG heartbeats, the PTT can also be measured. Afterwards, the SBP model can be firstly calibrated in the training session by a supervised learning process referring to the left arm cuff-based ground truth SBP, and then used for SBP estimation on the unseen data in the testing session.

1) Heart Rate Estimation

As mentioned above, the ECG signal is of a relatively better motion artifacts-tolerant ability than the PPG signal, therefore, the purified ECG heartbeats are used for instantaneous heart rate estimation. Then the windowed heart rate (denoted as HR, with a unit of beats-per-minute, denoted as BPM) estimates can be achieved, where the window corresponds to the second minute in each two-minute trial during which the SBP cuff is measured. The performance of the estimated HR will be evaluated in terms of mean error \pm standard deviation ($ME \pm STD$), mean absolute error (MAE) and root mean absolute error (RMSE).



2) Pulse Transit Time Calculation

Figure 2 Pulse transit time (PTT) measured with ECG and PPG signals (This illustration of PTT is based on ear-ECG/PPG signals).

Pulse transit time is the time consumed by the pressure pulse to flow from the proximal (PTT start time) to the distal (PTT end time) arterials sites. As shown in fig 2 the ECG R peak represents when the pulse leaves the proximal site, i.e., the thoracic aorta, and the PPG foot corresponds to when the pulse arrives the distal site. Similar to windowed HR, the instantaneous PTT measured in the second minute of each trial is also averaged to obtain the windowed PTT estimates. Pulse transit time (PTT) measured with ECG and PPG signal.

3) Blood Pressure Model Learning and Testing

Due to the complicated underlying blood pressure wave generation and propagation mechanisms, many SBP learning models have been reported based on diverse assumptions and strategies. To thoroughly compare them and determine an appropriate one for ear application scenarios, ten popular SBP learning models including seven PTT-SBP models, and three PTT&HR-SBP models with HR information enhanced. Among PTT-SBP models 1 to 7, various styles of equations are applied, such as linear, quadratic, exponential ones and so on, based on different deduction processes. For example, the model 2 reflects the reverse correlation between PTT and SBP shown by large amounts of studies, based on the fact that a high SBP will reduce the time consumed by the pressure pulse to propagate from the proximal to the distal sites, and vice versa. The model 7 is based on the combined action of the pulse wave and the energy of wave. Among PTT&HR-SBP models 8-10, the HR information is introduced to model establishment. They are based on the consideration that when HR increases, the cardiac output flow usually increased at the same time which causes a higher SBP, and vice versa. One thing worth noting is that, for simplicity and convenience purpose, the PPT measurement method introduced above actually includes another extra item, i.e., the pre-ejection period (PEP). PEP corresponds to the aortic valve opening time and usually significantly

increases the PTT measured. PEP can be measured by adding extra hardware components, such as the phonocardiogram (PCG) sensor or the impedance cardiography (ICG) sensor. Here, the PEP term is ignored for simplification purpose which is a common strategy used in many previous works. The HR information has been used to enhance the SBP model, therefore, we also consider PTT&HR-SBP models, for comparison purpose. The HR information is already carried by the ECG signal and no extra hardware components are needed. In future, new sensors can be added to measure PEP for further model enhancement. The SBP models are learned on the training data and tested on the unseen testing data to show the generalization ability. The left-arm cuff-based SBP is used as reference to enable a supervised learning process. The performance is reported in terms of $ME \pm STD$, MAE and RMSE

1) Heart Rate Estimation

As mentioned above, the ECG signal is of a relatively better motion artifacts-tolerant ability than the PPG signal, therefore, the purified ECG heartbeats are used for instantaneous heart rate estimation. Then the windowed heart rate (denoted as HR, with a unit of beats-per-minute, denoted as BPM) estimates can be achieved, where the window corresponds to the second minute in each two-minute trial during which the SBP cuff is measured. The performance of the estimated HR will be evaluated in terms of mean error \pm standard deviation ($ME \pm STD$), mean absolute error (MAE) and root mean absolute error (RMSE).

2) Pulse Transit Time Calculation

Pulse transit time is the time consumed by the pressure pulse to flow from the proximal (PTT start time) to the distal (PTT end time) arterials sites. As shown in Figure 2, the ECG R peak represents when the pulse leaves the proximal site, i.e., the thoracic aorta, and the PPG foot corresponds to when the pulse arrives the distal site, i.e., the skin

surface where the PPG sensor is placed on similar to windowed HR, the instantaneous PTT measured in the second minute of each trial is also averaged to obtain the windowed PTT estimates.

III. RESULT AND DISCUSSION

A. Signals Acquired

After situating the ECG electrodes behind two ears and the PPG sensor behind the left ear, our semi-customized bio-potential acquisition platform successfully collected the ear-ECG (fig 3a) and ear-PPG (Figure 3b) signals, where the chest-ECG signal is also given for comparison purpose. The acquired ear-ECG signal is only around 5% of the chest-ECG signal in terms of peak-to-peak voltage, resulting from a much smaller potential difference between the back locations of two ears. Although the ear-ECG is highly weak, it can still show distinguishable heartbeats, especially clear QRS complex morphologies, even with continuous background motion artifacts due to uncontrolled neck muscle and blood vessels movements, indicating the effectiveness of the proposed non-standard highly convenient single lead ECG configuration.

Meanwhile, the acquired PPG signal also owns a clear heartbeat morphology leveraging many blood vessels around the back location of the ear. When performing

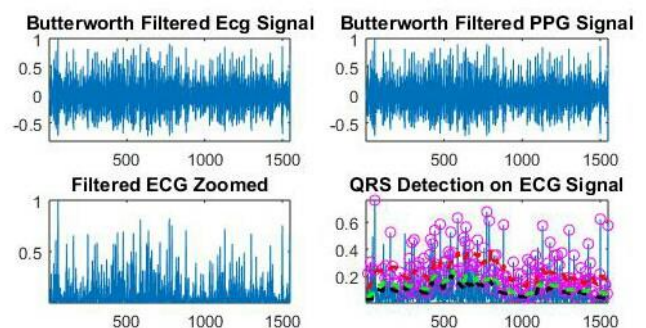


Figure 3

- i. Butterworth filtered ECG signal.
- ii. Butterworth filtered PPG signal.
- iii. Filtered ECG Zoomed.
- iv. QRS detection on ECG signal.

head movements, many motion artifacts are induced to both ear-ECG and ear-PPG signals (Figure 4d and 4b) which make heartbeats identification highly challenging. Therefore, advanced signal processing and machine learning algorithms for robust heartbeat recognition are proposed to enable this highly wearable ear signal acquisition solution .

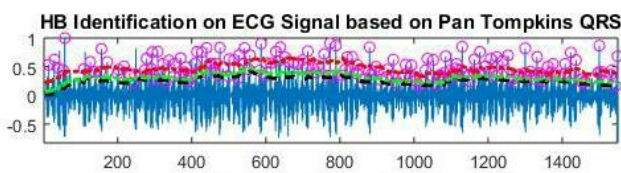


Figure 4. distortion quantification using threshold learning

Figure 4. An example of the signal segments acquired (chest-ECG, ear-PPG, and ear-ECG), showing that the weak ear-ECG has a peak-to-peak voltage only around 5% of that of the chest-ECG.

B. Heartbeat Identification

To identify raw heartbeats from motion artifacts-impacted or even corrupted ear signals, our previously proposed Pan Tompkins algorithm is applied on the weak ear-ECG signal. Heartbeat identification results in the testing session of subject 1 are given in Figure 4, where the raw ECG heartbeats are firstly identified and then the PPG heartbeats are determined by a simple minima searching method. There are several interesting observations as follows to support why we firstly identify the raw heartbeats from the ECG signal, and why we need to learn signal quality labelling based on the PPG signal in an unsupervised manner and purify both ECG/PPG heartbeats.

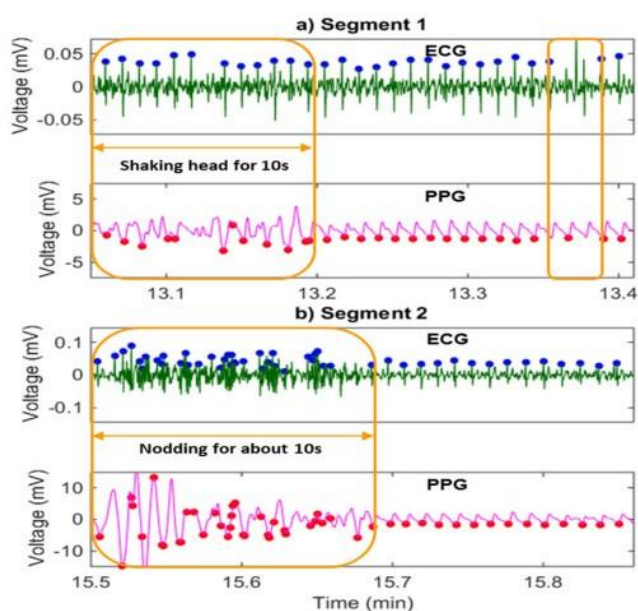
Firstly, the ECG signal acquired with the non-standard signal lead configuration is so weak that it

is continuously impacted by the background motion artifacts due to uncontrolled neck muscle and blood vessels movements. Specially, in the signal periods not covered by the wide orange rectangles, the PPG Figure 5 Heart Beat identification on ECG signal based on Pan-Tompkins QRS detection method signal owns a better signal morphology compared with the ECG signal, which is even highly corrupted by the background motion artifacts. Therefore, we firstly perform raw heartbeat identification from the ECG signal. Since PPG heartbeat morphological characteristics (PPG feet) during these signal periods cannot reflect the heartbeat occurrence time for PTT calculation, we need to filter out these signal segments according to the signal quality of these raw PPG heartbeats. Heartbeat identification results in the testing session of the subject 1. Blue dots: identified raw ECG heartbeat locations; red dots: identified raw PPG heartbeat locations; wide orange rectangles: signal periods with deliberately introduced motion artifacts due to head movements; narrow orange rectangle: signal period with missing or fake heartbeats due to severe background motion artifacts; all the weak ECG signal is continuously impacted by background motion artifacts. Based on these considerations, we choose an unsupervised learning approach to learn how to generate the SQI information for each raw PPG heartbeat.

C. PPG Segmentation and Template Learning

To perform unsupervised learning of signal quality labelling, we apply a DFT method to quantify the degree of distortion for each raw PPG heartbeat. The PPG template for the DFT method is learned by the K-medoids clustering approach on the segmented raw PPG heartbeats. The clustering results are given in Figure 5 where raw heartbeats with a relatively good quality concentrate in the M1 cluster, and raw heartbeats with a poor quality are grouped into many other clusters due to the high randomness induced by motion artifacts. Consequently, the medoid in cluster 12 which

represents a highest number of instances (#=65%, i.e., 65% of raw heartbeats in the second minute in the first trial are grouped into cluster 12) is selected as the high quality PPG heartbeat template. One interesting observation is that some slightly distorted heartbeats are also grouped into this cluster since the other clusters correspond to raw heartbeats so randomly corrupted by severe motion artifacts due to head movements. The high quality PPG template can still be well learned, because the K-medoids clustering algorithm makes each medoid represent the majority of instances in each cluster, i.e., minimizing the object-to-medoid dissimilarity as . Figure 5.



D. PPG Distortion Evaluation and Threshold Learning

After quantifying the degree of distortion for all raw PPG heartbeats using the DTW method, the histogram triangle-based approach is proposed for PPG distortion threshold learning which will be used to generate the SQI information. An example is given in Figure 6, where a skewed intensity histogram of the DTW distances is constructed. The relatively good quality heartbeats concentrate in the low distortion area (the left side of the x-axis) and poor quality heartbeats spread over a larger range resulting from high and diverse distortion values due to random and severe motion artifacts.

Figure 6 Figure 5. Two examples of heartbeat identification results in the testing session of the subject 1. Blue dots: identified raw ECG heartbeat locations; red dots: identified raw PPG heartbeat locations; wide orange rectangles: signal periods with deliberately introduced motion artifacts due to head movements; narrow orange rectangle: signal period with missing or fake heartbeats due to severe background motion artifacts; all the weak ECG signal is continuously impacted by background motion artifacts.

The global searching process effectively captures the transition point of the histogram and determines the normalized threshold $\hat{O}ST$ in this example as 0.07, which is then de-normalized and multiplied by a shrinkage factor to get the final distortion threshold ST which is 11.9 in this example. Figure 6.PPG distortion threshold learning in the first trial in the training session of subject 1. Blue line: the histogram hypotenuse; red curve: the histogram envelope; green line: the maximum perpendicular distance; green dot: the learned normalized (0-1 range) threshold.

E.SQI Generation and Heartbeats Purification

Based on the DFT distance-based distortion values and the learned distortion threshold, we now can generate the SQI information for all PPG raw heartbeats in the training or the testing session. The acquired thirty-minute ear-ECG and ear-PPG streams are shown in Figure 7a and 7b, where fifteen pink segments in each stream corresponding to the second minute in each of fifteen trials. In each pink segment, there is head shaking movement during the first ten seconds and nodding movement during the fourth ten seconds, resulting in many severe motion artifacts which increase the peak-to-peak voltage. In the last eight black segments, there are exercise-induced signal variations (riding the bike), especially in the ear-PPG stream. In the first seven black segments, there are also some signal variations due to normal head

movements. The calculated unsmoothed DFT distance and the smoothed one are given in Figure 7c, which shows diverse degree of distortion caused by both background and deliberately introduced motion artifacts. Based on SQI algorithm proposed, the distortion threshold is adaptively elevated if the best heartbeats need to be protected. Finally, the raw PPG heartbeat-specific SQI information is generated as Figure 8d. During deliberately introduced head movements (wide orange rectangles), the DFT distance-based distortion values (black bars) are much higher than those in other time periods. The smoothing operation of the distortion values can make the low distortion values above the distortion threshold and thus pose a more critical distortion evaluation during these highly suspicious periods (wide orange rectangles). On the other hand, the unsmoothed distortion values can still highlight the heartbeats with a high distortion condition (around minute 13.37).

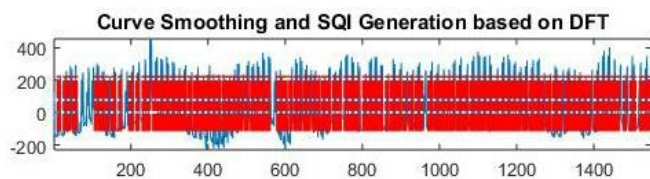


Figure 7. Curve smoothing and SQI Generation using DFT

Besides, the motion artifacts are so random that it is difficult to include all motion artifacts scenarios in the training session. If there happen to be some highly random motion artifacts. The corrupted PPG morphologies may induce dramatically high distortion values which generate a large range of suspicious period. This shows the necessity to introduce a protection mechanism to adaptively elevate the distortion threshold for some trials to protect the best (20%) heartbeats. Based on the proposed SQI generation algorithm, the raw heartbeats are labelled as accepted (SQI = 1) or rejected (SQI = 0), which helps filter out many signal segments highly corrupted by severe motion artifacts such that the remaining purified heartbeats

can be used in HR and PTT estimation later. Figure 7. The whole SQI generation process in the testing session of subject 1, including the signals acquired, quantified degree of distortion for raw PPG heartbeats, the adaptive distortion threshold and the SQI sequence generated

F. Heart Rate Estimation

The windowed heart rate estimates are achieved based on the ECG heartbeats. A Bland-Altman plot for estimated and reference HR is given in Figure 8 to illustrate the HR estimation performance. It shows that most of the HR estimates concentrate in the low error area, indicating the potential of using ear-ECG for robust long-term HR monitoring applications. Averaged over the acquired ear signal dataset, the $ME \pm STD$, MAE and RMSE of HR estimation are 0.8 ± 2.7 , 1.8 and 2.8 BPM, respectively. In table 2, the HR estimation performance using our approach greatly outperforms KLMF and DFT. For KLMF, a smoothing operation is applied to suppress the abnormal measurements based on the outlier indicators generated by the impulse rejection filter. However, the robustness of the outlier indicators is still very low due to the fact that the beat-to-beat checking rules used in this filter cannot effectively cover highly random cases due to large amounts of motion artifacts. For DFT, the low performance mainly suffers from the fact that the motion artifacts usually own a frequency spectrum highly overlapping that of the ECG signal. Therefore, there are still many residual motion artifacts in the reconstructed signal which lower the HR estimation performance

G. Blood Pressure Estimation

Based on HR and PTT estimates, ten diverse SBP models including seven PTT-SBP models (1-7) and three PTT&HR-SBP models (8-10) are thoroughly compared to explore their abilities in SBP estimation. According to the Advancement of Medical Instrumentation (AAMI) standard, the BP estimation

error should be less than 5.0 ± 8.0 mmHg in terms of mean error (ME) \pm standard deviation (SD). To thoroughly evaluate the SBP estimation performance, we consider four different criteria including ME, STD, MAE and RMSE. Moreover, although many wearable BP estimation studies only reported the performance on the training data, we test the proposed algorithm on the unseen testing data to emphasize the generalization ability of the learned SBP models. The performance comparison of ten SBP models and three signal processing approaches on the unseen testing data is summarized in Table 3. Using the proposed framework, model 8-10 effectively outperform model 1-7 leveraging the additionally introduced robust HR information, with the ME \pm STD, MAE and RMSE no more than -1.4 ± 5.2 , 4.2 and 5.4 mmHg, respectively. Compared with our framework, MLMF and DFT both show a worse performance due to the reason mentioned above, i.e., many residual motion artifacts. One thing worth noting is that model 8-10 for KLMF and DFT may even own worse performance than model 1-7, due to the introduction of low robust HR information into the BP models. To further illustrate the performance difference between the PTT-SBP models and the PTT&HR-SBP models. The latter one owns a smaller mean error and a more concentrated distribution (a smaller standard deviation) compared to the former one, indicating that the PTT-SBP model can be enhanced by the HR information, yielding a more robust PTT&HR-SBP model. On thing worth noting is that we have introduced exercise to perturb the BP to make the trained SBP model be able to cover a large range of BP (similar to many studies), and we did found strong correlations between heart rate and SBP (similar to the previous study), but more data acquisition protocols are also necessary considering that the relation between heart rate and SBP may need to be further explored.

IV. CONCLUSION

In this paper we propose monitoring of blood pressure and heart rate using Discrete Fourier Transform and

Pan Tompkins algorithm to achieve higher wear ability and high accuracy. Motion artifacts induced by the head movements are deals with machine learning framework to enable practical application scenarios. Here we suggest to place all the electrocardiography(ECG) and photoplethysmography(PPG) sensors behind two ears to successfully acquire weak ear -ECG/PPG signals using a semi customized platform. After introducing head motions towards ,we apply a unsupervised learning algorithm ,Pan Tompkins to learn and identify raw heartbeats from motion artifacts compacted signals. Further more, we propose another unsupervised learning algorithm to filter out distorted/faking heartbeats, for the estimation of ECG to PPG pulse transit time(PTT) and HR. Specifically, we introduce a Discrete Fourier Transform(DFT) to quantify distortion conditions of raw heartbeats referring to a high quality heartbeat pattern, which are then compared with a threshold to perform purification. The heartbeat pattern and the distortion threshold are learned by a K-medoids clustering approach and a histogram triangle method, respectively. Afterwards, we perform a comparative analysis on ten PTT or PTT&HR-based BP learning models. This study is expected to demonstrate the feasibility of the proof-of-concept system in wearable ear-ECG/PPG acquisition and motion-tolerant BP/HR estimation, to enable pervasive hypertension, heart health and fitness management. In future, we will acquire data from more subjects, and also further introduce motion artifacts from more scenarios, such as walking, running, sleeping, eating, etc. Another interesting work is to enhance the power efficiency of this easy-wearing blood pressure system for long-term wearable application scenarios.

V. REFERENCES

- [1]. L. Kaufman and P. J. Rousseeuw, "Partitioning around medoids(program pam)," Finding groups in data: an introduction to cluster analysis, pp. 68-125, 1990.

- [2]. Q. Zhang, C. Zahed, V. Nathan, D. A. Hall, and R. Jafari, "An ECG dataset representing real-world signal characteristics for wearable computers," in Biomedical Circuits and Systems Conference (BioCAS), 2015 IEEE, 2015, pp. 1-4.
- [3]. N. V. Thakor, J. G. Webster, and W. J. Tompkins, "Design, implementation, and evaluation of a microcomputer-based portable arrhythmia monitor," *Med. Biol. Eng. Comput.*, vol. 22, pp. 151-159, 1984.
- [4]. Jiapu Pan and Willis J Tompkins "A Real-Time QRS Detection Algorithm" *IEEE Transactions On Biomedical Engineering*, Vol. Bme-32, No. 3, March 1985.
- [5]. Q. Zhang, C. Zahed, V. Nathan, D. A. Hall, and R. Jafari, "An ECG dataset representing real-world signal characteristics for wearable computers," in Biomedical Circuits and Systems Conference (BioCAS), 2015 IEEE, 2015, pp. 1-4.
- [6]. F. S. Cattivelli and H. Garudadri, "Noninvasive cuffless estimation of blood pressure from pulse arrival time and heart rate with adaptive calibration," in 2009 Sixth international workshop on wearable and implantable body sensor networks, 2009, pp. 114-119.
- [7]. X. Long, P. Fonseca, J. Foussier, R. Haakma, and R. M. Aarts, "Sleep and wake classification with actigraphy and respiratory effort using dynamic warping," *IEEE journal of biomedical and health informatics*, vol. 18, pp. 1272-1284, 2014.